



1
2
3
4
5
6
7
8
9
10
11
12
13
14
15
16
17
18
19

**Evaluating robustness of dynamic reservoir management under
diverse climatic uncertainties: Application to the Boryeong
Reservoir in South Korea**

Kuk-Hyun Ahn¹ and Young-Il Moon²

20 ¹Assistant Professor, Department of Civil and Environmental Engineering, Kongju National
21 University, Cheon-an, South Korea; *Corresponding author*; e-mail: ahnkukhyun@gmail.com

22 ² Professor, Department of Civil Engineering, University of Seoul, Seoul, South Korea; e-
23 mail: ymoon@uos.ac.kr



24

25

ABSTRACT

26

27 The implications of forecast-based reservoir operation have been considered to be innovative
28 approaches to water management. Despite the advantages of forecast-based operations,
29 climate-related uncertainty may discourage the utilization of forecast-based reservoir operation
30 in water resources management. To mitigate this concern, a systematic evaluation proves
31 helpful. This study presents an evaluation framework for reservoir management under a variety
32 of potential climate conditions. In particular, this study uses Monte Carlo simulations to
33 quantify the robustness of the forecast-based operation in a scenario of degraded ability of
34 forecast skill, and demonstrates a new performance metric for robustness. This framework is
35 described in a case study for a water supply facility in South Korea. To illustrate the framework,
36 this study also proposes dynamic reservoir operation rules for our case study, utilizing seasonal
37 climate information and a real-option instrument from an interconnected water system. Results
38 provide system robustness evaluated over a wide range of defined uncertainties related to
39 climate change. Results also suggest that the dynamic operation management adopted in this
40 study can substantially improve reservoir performance for future climates compared to current
41 operation management. This analysis may serve as a useful guideline to adopt dynamic
42 management of reservoir operation for water supply systems in South Korea and other regions.

43

44 **Keywords:** Dynamic reservoir operation, Climate change, Robustness, Boryeong

45

Reservoir

46

47



48 **1. Introduction**

49 Population growth, resultant water demand, and recent climate change have increased the
50 likelihood of water deficits in many regions of the world (Padowski et al., 2015; Schewe et al.,
51 2014). Efficient of hydrologic infrastructure is required to cope with present and future
52 uncertainty (Ahmad et al., 2014). To meet these demands, considerable improvement in water
53 resources system operations has been achieved over the last decade, including multi-objective
54 operations (Tsai et al., 2015; Yang et al., 2015), the use of inflow forecasts (Giuliani et al., 2015;
55 Sankarasubramanian et al., 2009), conjunctive use with groundwater (Liu et al., 2013; Singh et
56 al., 2015), and optional transfers from an adjunct system (Jeuland and Whittington, 2014;
57 Palmer and Characklis, 2009).

58

59 The utility of forecasts in reservoir operations has long been investigated (e.g., Bai et al., 2014;
60 Giuliani et al., 2015; Yao and Georgakakos, 2001; Zhao et al., 2012). To manage interannual
61 hydrologic oscillation, seasonal climate forecasts (1-6 months) have been often coupled with
62 reservoir operations (Block, 2011; Gong et al., 2010; Najibi et al., 2017; Sankarasubramanian
63 et al., 2009; Steinschneider and Brown, 2012). These forecast-based operations are notably
64 beneficial to conserve water supplies during low-flow periods (Block, 2011; Golembesky et al.,
65 2009). Despite the advantages of forecast-based operations, the possibility of forecast skill
66 degradation diminishes their utility in water resources management. Forecast skill degradation
67 indicates that predictive ability is decreased when an adopted covariate (e.g., climate
68 teleconnection) is utilized for estimating inflow in a reservoir. To better assess this concern, a
69 systematic approach is required to assess the impact of the possibility of forecast skill
70 degradation on the reliability of forecast-based operations, which has received little attention



71 in previous studies. This study supports the field of reservoir operations by proposing a
72 framework to examine how altered forecast skills could influence the behavior of system design.

73

74 To achieve the primary objective, we newly identify a useful seasonal climate pattern, which
75 can be utilized to develop seasonal climate-based operations for the study's water supply
76 facility. Seasonal climate-based operations and their climate covariates are becoming more
77 widely suggested in many reservoir systems in many regions seeking multiple objectives
78 (Broad et al., 2007; Gong et al., 2010; Najibi et al., 2017; Steinschneider and Brown, 2012).
79 Also, seasonal climate-based operations have been considered as improved system operation
80 rules (Block, 2011; Visser, 2017). Because the impacts and roles of climate covariates are
81 diverse depending on geographical location (Ashbolt and Perera, 2018), reservoir operations
82 incorporating teleconnections from large-scale atmospheric oceanic circulation patterns must
83 pertain specifically to each system. To be tailored for our water supply facility, a forecast-based
84 operation algorithm is also described to incorporate the large-scale oceanic circulation pattern
85 identified in this study. Following Gong et al. (2010) and Steinschneider and Brown (2012),
86 forecast information is used to determine water rationing to circumvent severe shortfalls by
87 diminishing the normal supply.

88

89 Climate-based operations have further been used as reliable climate change adaptation
90 strategies (Steinschneider and Brown, 2012; Whateley et al., 2014). However, as noted by
91 Romsdahl (2011) and Whateley et al. (2014), water resource managers may not be receptive to
92 the use of forecast-based reservoir operations for their long-term operation plans (i.e., climate
93 change adaptation plans) for various reasons such as financial constraints, insufficient skill,



94 and institutional obstacles. In particular, the possibility of forecast skill degradation may be one
95 of the main reasons for this reluctance. Global climate change may accelerate unexpected
96 alterations in the relationship between large-scale synoptic circulation and local hydrology. For
97 instance, Allan et al. (2014) describe possible changes in future surface hydrology related to
98 the Pacific-North American (PNA) teleconnection pattern. A similar interpretation can be found
99 for ENSO with local hydrology (Kohyama et al., 2018). In these cases, a forecast with
100 unreliable predictions may lead water managers to make inappropriate operation decisions,
101 resulting in subsequent critical shortages and severe criticism from stakeholders. One possible
102 way to mitigate this concern is to explicitly evaluate the impacts of changes in forecast skill in
103 the relationship between large-scale synoptic circulation and local hydrology by
104 simultaneously considering potential shifts in climate. Such an evaluation may identify
105 adequate bounds ensuring acceptable performance at a reasonable risk.

106

107 The impact of climate change on water resources management has been widely investigated
108 (Zhang et al., 2017). Global circulation models (GCMs) are commonly employed for
109 understanding potential shifts in climate, but due to biases and incomplete sampling of
110 uncertainties, they are limited for risk assessments exploring potential climate change (Brown
111 and Wilby, 2012). Poorly understood climate physics and computational complexity further
112 exacerbate limitations in incorporating information from these scenarios into climate change
113 assessments (Koutsoyiannis et al., 2009). Alternatively, robustness-based methods have been
114 proposed without direct use of climate model projections, focusing on analysis that quantifies
115 the range of climate space over which a water resource system can provide acceptable
116 performance. Examples include info-gap analysis (Korteling et al., 2013), robust decision
117 making (Lempert and Groves, 2010; Matrosov et al., 2013) and decision scaling (Brown et al.,



118 2012; Turner et al., 2014). The robustness-based method has been increasingly used to assess
119 system vulnerability and to propose alternative policy decisions (Brown et al., 2011; Ghile et
120 al., 2014; Hassanzadeh et al., 2016). Based on the robustness-based method (decision scaling
121 is adopted in this study), we develop an evaluation framework to systematically account for
122 uncertainties related to internal climate variability when determining if altered forecast skills
123 are reliable.

124

125 In South Korea, drought risk has not been an explicit concern as an increase in precipitation
126 over South Korea has been documented in various studies (Ho et al., 2003; Kim and Jain, 2011;
127 Lee et al., 2012). However, many regions of Korea have recently been experiencing water
128 deficit (Kwon et al., 2016). To be specific, the Korean peninsula experienced severe droughts
129 in 2002 and 2014-2016 (Kim et al., 2018). During the 2014-2016 drought, local water managers
130 executed water supply restrictions for many areas of the west coast of South Korea, thereby
131 adversely affecting the environment and living conditions for people (Ihm et al., 2019). This
132 multi-year drought drew water managers' attention in South Korea because it was an
133 exceptional event considering the regularly recurring flood season (June to August) every year.
134 Multi-year drought poses a new and substantial challenge to water managers deciding current
135 strategies to ensure prudent future reservoir operations.

136

137 Cognizant of the risk of a multi-year drought, local water managers in South Korea have
138 constructed real-option water transfers enabling offsetting local water shortfalls by drawing
139 water from distant water resource systems. For example, the Korean Water Resources
140 Corporation (K-water) recently constructed a water transfer pipe from the Baekje Weir to the



141 Boryeong Reservoir in anticipation of water shortages (Kim et al., 2017). Although many
142 studies have advocated the use of option instruments for mitigating water resource system
143 failures (Palmer and Characklis, 2009; Zeff et al., 2016; Zhu et al., 2015), many scientists in
144 South Korea question whether water transfer options are valuable (Jang et al., 2017). However,
145 even if water transfers may not be worthwhile for the present, they could prove promising in
146 the face of unexpected future climate conditions. Accordingly, we utilize the proposed
147 framework to investigate the utility of water transfer options for both the present and a future
148 with climate change. We also examine if more effective water management would result during
149 critical drawdowns when water transfer is utilized concurrently with our new climate-based
150 operation curve.

151

152 In summary, this study seeks to answer the following questions in a case study of daily
153 streamflow for water supply facilities (the Boryeong Reservoir and Baekje Weir) in South
154 Korea. The water supply facilities recently experienced the worst drought in the historical
155 record, highlighting that reliable and effective operation rules are urgently required for both the
156 present and the future.

157

- 158 1. Can a forecast-based operation rule improve performance for the Boryeong Reservoir
159 compared to the status quo operation rule?
- 160 2. Will the real-option water transfer installed between the Baekje Weir and the Boryeong
161 Reservoir prove useful to curtail water shortages? What are the potential contributions
162 of real-option water transfer when utilized concurrently with our operation rule?



163 3. If the dynamic operation rule was adopted, how responsive would our improved
164 reservoir system be under long-term climate change as well as changes in seasonal
165 forecast skill?

166

167 The rest of this paper is described as follows. Section 2 delineates a theoretical background of
168 the dynamic reservoir operation and the proposed framework. Section 3 introduces a specific
169 application to the Boryeong Reservoir system, the primary water supply system for Boryeong
170 in South Korea. Results are presented in section 4. The paper concludes with a discussion of
171 some limitations of our approach as well as potential research needs in section 5.

172

173 **2. Methodologies**

174 In this study, the methodology is comprised of three major components. The first follows
175 Steinschneider and Brown (2012) to develop dynamic reservoir management incorporating
176 forecast-based operations and real-option water transfer from an interconnected water system
177 (Section 2.1). We then present how to generate future streamflow scenarios using a stochastic
178 weather generator and a hydrologic model (Section 2.2). Finally, we introduce a new
179 framework using Monte Carlo methods to explore whether different operation rules provide
180 appropriate performance over a wide array of uncertainties (Section 2.3). To be specific, three
181 reservoir operation rules are evaluated. The first rule $C_{Baseline}$ presents a baseline and status
182 quo operation, comparable to that currently used in our study case. The second rule $C_{Forecast}$
183 employs forecast-based operations without the ability to hedge risk with a real-option. The real-
184 option from an interconnected water system is then added to bolster the dynamic operation in



185 the third rule $C_{Dynamic}$. Following Field et al. (2012), robustness is defined when an operation
186 plan performs well across many feasible scenarios. Accordingly, the operation rule options can
187 be robust to a specific type of long-term alterations if they produce an acceptable performance
188 for overall simulations associated with that long-term alteration. A detailed explanation of each
189 step is provided in the following sections.

190

191 2.1 Dynamic reservoir management

192 The operation rule curve C can be formalized as $C = f(Q)$, where C is a set of daily
193 reservoir storage levels, Q is a set of daily inflow sequences, and $f(\cdot)$ represents the function
194 used to derive the rule curve. Each inflow sequence q covers one calendar year with total n
195 years. The dynamic operation rule is designed for d different phases of a climate
196 teleconnection utilized for forecast use. To be specific, the historical record is divided by year
197 into d mutually exclusive sets, Q_1, \dots, Q_d such that for all years in a given set, the climate
198 index is in one particular phase.

199

$$200 \quad Q_d = \{q_{\tilde{n}} | \tilde{n} \in \tilde{N}_d\} \quad (\text{Eq. 1})$$

$$201 \quad \tilde{N}_d = \{\tilde{n} | I_{\tilde{n}} \in (i_d, \lambda_d), \tilde{n} \in [1, 2, \dots, N]\} \quad (\text{Eq. 2})$$

202

203 where, $I_{\tilde{n}}$ is an index measuring climate teleconnection for the \tilde{n} calendar years in the
204 historic record, i_d and λ_d indicate minimum and maximum values, respectively, to delimitate
205 the d^{th} phase of the climate conditions, and Q_d is a set of inflow that occurred during years



206 for the d^{th} phase of the climate conditions. To drive the dynamic operation rule, inflow
207 sequences are limited to Q_d associated with that particular phase of climate variability $C_d =$
208 $f(Q_d)$.

209

210 During real-time operations, forecast-based operations are maintained for one calendar year.
211 The month following the release of climate information, reservoir operations are altered
212 corresponding to the rule curve obtained by the current phase of the climate information. After
213 one calendar year, the reservoir operation is changed by the new forecast. Note that the forecast-
214 based operation applied in this study is relatively straightforward. Perhaps monthly updating
215 of the rule curve could be more promising as noted in Aboutaleb et al. (2015).

216

217 The specific dynamic operation rule associated with that particular phase of climate variability
218 (C_d) is determined by a stochastic analysis. The methodology of a stochastic analysis is
219 described in detail elsewhere (Steinschneider and Brown, 2012; Westphal et al., 2007) so is
220 only briefly reviewed here. At its core, C is defined such that it has a certain chance that a
221 reservoir system is drawn down below the critical storage level C^{***} over a period given
222 different initial reservoir conditions and time of year. C is designed across time by month so
223 is constant for all period in a given calendar month. To consider the multi-year drought,
224 resampled two year sequences of inflow, drawn from a set of yearly inflow sequences, are
225 utilized. After identifying the minimum-maximum storage levels for the certain chance,
226 linearly interpolation is employed between the two minimum-maximum storage levels for each
227 month.



228

229 In addition, water transfer (TR) from an interconnected water system is operated during specific
230 periods when the storage level of the target reservoir falls below a certain storage level (C^{**}
231 used in this study). The decision rule to facilitate the option is formulated as

232

$$233 \quad TR_t = \begin{cases} \min(C^{**} - S_{t-1}, TR_{max}) & \forall S_{t-1} < C^{**} \\ 0 & \forall S_{t-1} \geq C^{**} \end{cases} \quad (\text{Eq. 3})$$

234

235 where S_{t-1} is the reservoir storage at $t-1$ and TR_{max} is the maximum volume of water which
236 can be transferred from the interconnect water system. Here, the amount of water transferred
237 in the option is designed as a function of how far the current storage falls below the predefined
238 storage C^{**} and is limited by physical constraints (e.g., maximum pipe volume).

239

240 *2.2 Future inflow realization under climate alternatives*

241 The operation rule curve is evaluated through an exhaustive sampling of changes in climate
242 variables, such as mean precipitation and temperature changes. A weather generator developed
243 by Cordano and Eccel (2016) is used to provide climate sequences that exhibit similar climate
244 statistics. To be specific, daily precipitation, maximum, and minimum temperatures are
245 generated for each specified mean climate future in this study. The weather generator utilizes
246 a vector autoregressive (VAR) model (Pfaff, 2008) to preserve temporal and spatial correlations
247 among generated daily precipitation and temperatures. The auto-regression order must be



248 determined prior to scenario generation, and is decided based on the AIC (Akaike, 1981)
249 calculated from the observed data. Then the VAR model is calibrated on the transformed time
250 series which is transformed into Gaussian-distributed random variables through
251 deseasonalization and Principal Component Analysis (PCA). Details on the methodologies
252 about the weather generator can be found in Cordano and Eccel (2016).

253

254 Climate sequences can be developed over any range of potential climate change. While the
255 selection of this range remains still an open question, the range can specify a large sufficient
256 range that can cover the climate space that is explored by GCM projections and ensure that the
257 endpoints of the range do not emerge in a meaningful implication (Whateley et al., 2014). Also,
258 a number of climate simulations (e.g., 100-1000) are needed to adequately explore possible
259 climate fluctuations (Guimarães and Santos, 2011). Following these two logical strategies, 40-
260 year daily simulations of climate are generated 200 times with different climate changes
261 imposed on the mean of precipitation and maximum/minimum temperatures in this study.
262 Climate changes include percent changes in mean precipitation (−25% to 30% in 5%
263 increments) and absolute changes in mean maximum and minimum temperatures (−2.0°C to
264 2.0°C in 0.5°C increments) from baseline values. Therefore, $21600 = 200 \times 12 \times 9$
265 different 40-year climate sequences are developed in this study.

266

267 A conceptual, lumped parameter hydrologic model, the Sacramento Soil Moisture Accounting
268 (SAC-SMA) model (Burnash, 1995; Burnash et al., 1973) is used to simulate future daily
269 streamflow from the generated climate sequences. The SAC-SMA divides the basin into two
270 soil zones, an upper zone and a lower zone, which is its most representative feature compared



271 to other typical hydrologic models (e.g., PRMS, VIC, and HBV). The upper zone simulates the
272 short-term storage of the basin; the lower zone represents the underground soil in the long-term
273 storage. Each zone is affected by evapotranspiration and free water, thereby representing the
274 water that evaporates and the water that flows or percolates downward (Najafi et al., 2011).
275 The generation processes are delineated by a total of 16 unknown parameters, but 3 parameters
276 (SIDE, RIVA, RSERV) are set to their default values as in other studies (e.g., Chu et al. (2010)),
277 leaving 13 parameters for calibration. In addition, effective rainfall and snowmelt input to
278 SAC-SMA is considered to simulate snow accumulation/melting processes using a snow model
279 similar to those of Ahn et al., (2016a) and Martinez and Gupta (2010) based on daily mean
280 temperature, with an additional 3 parameters. Lastly, to account for biases in climate variables,
281 an input data error model is employed based on two formulations, a multiplier form (Li and
282 Xu, 2014) and an additive form (Huard and Mailhot, 2006), which have been widely applied
283 (Jin et al., 2010; Zhang et al., 2016). Errors in temperature (precipitation and evapotranspiration)
284 is assumed to be additive (multiple) which can be formulated as follows:

285

$$286 \quad \widehat{T}_t = T_t + e_T$$

$$287 \quad \widehat{P}_t = P_t e_P \quad \text{Eq. (4)}$$

$$288 \quad \widehat{PET}_t = PET_t e_{PET}$$

289

290 where e represents the bias correction term for temperature (T), precipitation (P), and
291 evapotranspiration (PET). The Hargreaves method (Hargreaves and Samani, 1982) is used for
292 estimating PET from maximum and minimum temperatures. Radiation values for the



293 Hargreaves method are estimated by the method proposed by (Allen et al., 1998).

294

295 In total, the 19 parameters of the model (presented in Table 1) are calibrated by maximizing
296 Kling-Gupta efficiency (KGE; Gupta et al., 2009) using the differential evolution optimization
297 algorithm (Mullen et al., 2009). KGE (ranging between $-\infty$ and 1) is composed of three
298 independent error components, including terms for mean bias, variability bias, and correlation
299 between the simulated and observed flows. This performance metric has advantages over
300 traditional skill measures like Nash-Sutcliffe efficiency (NSE) because it removes interactions
301 between error components and reduces negative variability bias in simulation results (Revilla-
302 Romero et al., 2015).

303

304 *2.3 Framework to evaluate robustness of diverse alternatives*

305 The framework focuses on demonstrating how robust the alternatives of forecast skills function
306 under various potential climate conditions. To be specific, we evaluate a reservoir plan under
307 three alterations in climate (changes in precipitation, temperatures and seasonal forecast skills
308 related to teleconnection). A plan is considered robust to a set of alterations if it offers satisfying
309 performance for overall Monte Carlo simulations related to the three alterations. Although three
310 climate-related alterations are considered here, the framework can be easily expanded to
311 consider other feasible alterations such as changes in water supply demands.

312

313 The following procedure is used to define robustness in this study.



314 [1] For a reservoir operation plan, $g = 1, \dots, G$ future precipitation, maximum and minimum
315 temperatures are generated under each long-term climate change scenario under $h = 1, \dots, H$.
316 In this study, $G = 200$ climate sequences are produced under $H = 117$ change scenarios (as
317 stated in Section 2.2). Thereby, G streamflow simulations are obtained for each long-term
318 change scenario.

319 [2] For each of $j = 1, \dots, J$ conditions of forecast skills, a future teleconnection index is
320 developed by a bivariate conditional expectation with the generated streamflows. Here, the
321 forecast skill ability is defined by the correlation ($\rho_{i\tilde{q}}$) between the seasonal index value (\tilde{i}) and
322 the generated seasonal streamflows (\tilde{q}). Therefore, future seasonal values of the forecast-
323 informed index are generated by $N(\mu_{\tilde{i}} + \frac{\sigma_{\tilde{i}}}{\sigma_{\tilde{q}}} \rho_{i\tilde{q}}(\tilde{q} - \tilde{i}), (1 - \rho_{i\tilde{q}}^2)\sigma_{\tilde{i}}^2)$. In this study, $J = 5$
324 future forecast skills are generated to examine the impacts of forecast skill degradation, along
325 with G streamflow simulations for each long-term change (illustrated in Section 4.1).

326 [3] After a reservoir plan is operated with future streamflow simulations, a binary performance
327 score, $U(h, g, j)$, is developed to characterize system performance. The binary performance
328 score returns a value of 1 if the reservoir operation shows acceptable performance; otherwise
329 it obtains a value of 0. In this study, performance is considered acceptable if simulated storages
330 S_t are maintained above a predefined threshold (the critical storage C^{***} used here is
331 described in Section 3.1). Instead, acceptable performance can be defined by comparing any
332 performance variable (e.g., deficit in water supply) with a predefined threshold.

333 [4] For h^{th} long-term climate change scenario and j^{th} condition of forecast skill, the
334 robustness index (RI) of the specific reservoir operation, similar to (Steinschneider et al., 2015),
335 is developed by integrating the binary performance scores (Eq. 5).



336

$$337 \quad RI_{h,j} = \frac{1}{G} \sum_{g=1}^G U(h, g, j) \quad \text{Eq. (5)}$$

338

339 In this study, averaging binary scores is used to summarize a sufficiently large number of future
340 scenarios ($G = 200$). We note that an additional process (e.g., providing a different weight to
341 each scenario) may be considered to develop the RI if limited sets of scenarios are used. Then,
342 assigning normalized weights for each scenario can be used.

343 Although other performance metrics are available (e.g., reliability, resilience, and vulnerability
344 described in Fowler et al. (2003) and Hashimoto et al. (1982)), the RI is preferred in this study
345 because the three metrics may be more appropriate under conditions where the single time
346 series is believed to fully represent the uncertainty of future inflows but is less appropriated in
347 the analysis with many possible future scenarios (Whateley et al., 2014).

348 [5] The RI offers a mapping, which can be used to determine whether a reservoir plan is robust
349 under potential climate conditions considered. If the RI for the defined climate condition is
350 greater than the adequate threshold ($\Lambda^{RI} = 0.9$ in this study), we consider the reservoir plan
351 robust for the climate condition. In addition, an ensemble of GCM projections is superimposed
352 on these surfaces to provide the likelihood of different climate changes.

353 [6] Finally, the degradation robustness index (DRI) of the forecast-based reservoir operation is
354 developed under j^{th} forecast skill change as follows:

355



356
$$DRI_j = \frac{1}{G \times H} \sum_{h=1}^H \sum_{g=1}^G U(h, g, j)$$
 Eq. (6)

357

358 Similar to the RI, an adequate threshold is defined for the DRI ($\Lambda^{DRI} = 0.7$ in this study).

359 Although this threshold is arbitrary, it is quite useful in a decision-making process. Also, the

360 lower threshold is acceptable because it must consider a plan under a sufficiently large range

361 of long-term climate change scenarios. Alternatively, system planners can decide the value of

362 the threshold based on their expertise after reviewing the robustness.

363

364 **3. Case Study Description**

365 *3.1 Overview of water supply system and its rule curve*

366 This study focuses on the water supply systems in two adjacent basins including the Geum

367 River Basin and the western Geum River Basin, located in midwest of South Korea (Figure 1).

368 The basins receive an annual average of 1,250 mm precipitation. Similar to other regions in

369 South Korea, the basins are affected by a monsoon climate that often generates extraordinarily

370 heavy rainfall and corresponding floods in the summer (Yan et al., 2015). Accordingly, two-

371 third of annual precipitation is concentrated in the summer spanning from June to early

372 September (flood season) while only one-thirds of annual precipitation falls during the

373 remaining months (drawdown season). The drawdown season is generally dry, contributing to

374 periodic droughts to the basins (Ahn and Kim, 2019). These distinct seasonal climate

375 fluctuations pose significant water management challenges including requiring deliberate

376 operation of the local reservoirs (Sohn et al., 2013).



377

378 This study uses the Boryeong Reservoir in the western Geum River Basin, and the Baekje Weir
379 in the Geum River Basin (Figure 1). The Boryeong Reservoir with a storage capacity of 116.9
380 MCM (1 MCM is equal to 10^6 m^3) was constructed in 1998 to serve four main purposes: (1)
381 flood control, (2) water supply, (3) water quality, and (4) hydropower generation, and is
382 operated by the Korean water resources corporation (K-water). The reservoir serves as the
383 principal municipal and industrial water supply (WS^M) source for eight cities such as Boryeong,
384 Dangjin, and Seosan, and is also operated for hydropower generation (WS^{HP}), environmental
385 demand (WS^{EN}), and supply of seasonal irrigation demand (WS^{IR}). Therefore, total controlled
386 releases for water supply at time t are expressed as $R_t = W \xi^M + W \xi^N + W \xi^R + W \xi^{HP}$.
387 While the reservoir has a flood control storage capacity (106.3 MCM) for the flood season, the
388 dead storage capacity is limited to 8.1 MCM for the drawdown season.

389

390 Our study basin experienced severe droughts in 2002 and 2014-2016. In particular, during the
391 2014-2016 drought, the Boryeong Reservoir failed to satisfy the designed demands including
392 municipal, agricultural, and environmental water supplies, adversely affecting the environment
393 and inadvertently harming people. During the multi-year drought, storage of the reservoir was
394 depleted to just 18.9% of its capacity—which is the minimum percentage in the historical
395 record (Hong et al., 2016). To protect the system against other extreme droughts and changes
396 in climate, two alternatives have been suggested. First, a new operation rule, comprised of three
397 storage levels, was developed for the Boryeong Reservoir (Figure 2; Ministry of Land,
398 Infrastructure and Transport, 2015). If the reservoir level drops below the mild storage level C^* ,
399 water allocation for WS^{EN} is terminated the water level rises above C^* . Then, if the reservoir
400 level falls below than the severe level C^{**} , three water demands (WS^{EN} , WS^{IR} , WS^M) are



401 restricted by 100%, 30% and 10%, respectively. Here, additional water restriction of 10% is
402 conducted for WS^{MI} if the reservoir level drops below the critical storage level C^{**} . In the
403 analysis, we adopt the water restriction policies across the three operation rules (C_{Base} ,
404 $C_{Forecast}$, $C_{Dynamic}$). Also, the current critical level C^{**} is employed to make a fair
405 comparison between strategies whereas C^* and C^{**} of the forecast-based operations are
406 determined by a stochastic model (see Section 2.1).

407

408 Next, K-water recently constructed a 21 km, 110 cm water transfer pipe connecting the Baekje
409 Weir (storage capacity: 28.7 MCM) to the Boryeong Reservoir in preparation for water
410 shortages. The Baekje Weir was completed in 2013 to mainly support agricultural demand with
411 the flood control storage capacity (28.6 MCM) and dead storage capacity (5.7 MCM). The new
412 pipe can draw water from the Baekje Weir with a maximum of 115,000 m³ per day before
413 depleting storage of the Boryeong Reservoir. For this strategy, the water transfer option is
414 triggered when storage of the Boryeong Reservoir falls below the severe level C^{**} and
415 continues until the Boryeong Reservoir rises above C^{**} .

416

417 Finally, the storage (S) of the Boryeong Reservoir can be formulated as follows:

418

$$419 \quad S_t = S_{t-1} + q_t + TR_t - SP_t - R_t \quad \text{Eq. (7)}$$

420

421 where SP_t indicates any water that spills out from the reservoir. We define that SP_t occurs
422 only when $S_t > S_{max}$

423

424 *3.2 Data*



425 Historic daily climate data, including precipitation, maximum and minimum temperatures were
426 gathered from 60 of the Korea Meteorological Administration's Automated Surface Observing
427 System (ASOS) gauges. The climate data was interpolated onto a 1/8 degree resolution (~140
428 km²) by using the Thiessen polygons (Thiessen, 1911). The final historic data set was obtained
429 over the period of 1 January 1973 to 31 December 2018 by averaging the values within the grid
430 cells overlapping our study basin areas. In addition, monthly sea surface temperatures (SSTs)
431 were obtained from the Extended Reconstructed Sea Surface Temperature version 5
432 dataset (Huang et al., 2017).

433

434 Daily historical inflow data for the Boryeong Reservoir was gathered online from the "Water
435 Resources Management Information System" webpage (<http://www.wamis.go.kr/>) for the
436 period of 1 January 1998 to 31 December 2018. The same hydrologic dataset for the Baekje
437 Weir was collected from the "My water" webpage (<http://www.water.or.kr/>) over the period
438 between 1 January 2013 and 31 December 2018. Note that both sets of hydrologic data were
439 available only upon completion of their construction, respectively. Current demand data for all
440 water use were obtained from our partners in K-water.

441

442 Mean changes in precipitation and maximum/minimum temperatures were collected from the
443 World Climate Research Programme's Coupled Model Intercomparison Project Phase 5 (CMIP
444 5) multimodel data sets. The climate model projections were bias corrected using the detrended
445 quantile mapping (DQM; Bürger et al., 2013; Eum and Cannon, 2017) method. These projected
446 changes in precipitation and temperatures were calculated across the entire Boryeong Basin
447 using 30-year windows between 1976 and 2005 (baseline) and 2051 and 2080 (future). Two
448 emission scenarios (Representative Concentration Pathways 4.5 and 8.5) and initial condition



449 members of 26 models (presented in Table S1) were employed in the analysis.

450

451 **4. Results**

452 *4.1 Climate teleconnections for Boryeong Reservoir*

453 Many studies have well documented the global impacts of the El Niño-Southern Oscillation
454 (ENSO), a large-scale oceanic circulation pattern in the tropical Pacific Ocean (Kug et al., 2009;
455 Sharma et al., 2016; Ward et al., 2014) whereas further examination is necessary to investigate
456 its effects on the Korean Peninsula (Yoon and Lee, 2016). We identify that ENSO exhibits a
457 lagged influence over hydroclimate in the western Geum River Basin and is used to construct
458 hydrologic forecasts for the region during early spring, the most crucial period for reservoir
459 operation in drawdown season. Figure 3a shows the Pearson correlation coefficients between
460 June-August (JJA) SST at each ocean grid cell and average February-April (FMA) streamflow
461 in the coming year for the Boryeong Basin over the period of 1998-2018 (21 years). Similar
462 analysis is conducted for seasonal low flows defined here by seasonal 20 day low flows (Figure
463 3b). These correlation patterns reveal that the FMA inflows are significantly and positively
464 related with lagged ENSO, implying that summer ENSO provides some predictability. Wang
465 and Fu (2000) reported that during El Niño, an anticyclonic flow over the Philippine Sea
466 develops, intensifying during the previous seasons and can affect climate in the following
467 winter, bringing warm and moist air to East Asia. Following this pattern, hydrologic conditions
468 are wetter (drier) than usual with lagged effect during El Niño (La Niña) events in our study
469 area. For simplicity, we use Niño 3.4 (Gergis and Fowler, 2005) to represent the magnitude of
470 ENSO (Figures 3c and 3d). The correlation (ρ) between Niño 3.4 and seasonal average flows
471 (seasonal low flows) is 0.72 (0.58), indicating that the relationship is fairly significant. For



472 developing forecast-based operations, the binary forecasts of Niño 3.4) are issued based on the
473 state of the Niño 3.4 indices being greater than or less than median values (Niño 3.4⁺ and
474 Niño 3.4⁻) in this study. Also, seasonal low flows are utilized to investigate the potential
475 impacts of forecast skill change from the relationships with Niño 3.4 because seasonal low
476 flows are more directly associated with drought conditions than average flows. Accordingly,
477 future forecast skills ($J = 5$) of Niño 3.4 are defined by absolute changes in the correlation
478 with seasonal low flows (ranges between 0.15 and 0.75).

479

480 *4.2 Performances of weather generator and hydrologic modeling*

481 Figure 4 shows a brief evaluation to demonstrate the ability of the weather generator to simulate
482 historical climate conditions for the Boryeong and Beakje Basins. Here, 400 simulations with
483 no changes imposed are compared against observed statistics for each calendar month. The
484 average, standard deviation, skew of daily precipitation, and kurtosis of daily precipitation are
485 displayed in Figure 4a-d. Similarly, the average and standard deviation of maximum/minimum
486 temperatures are presented in Figure 4e-f. Overall, the results suggest good performance for all
487 variables and statistics with observation values falling within the range of the simulations. Note
488 that the simulations are slightly biased in regard to standard deviations of maximum/minimum
489 temperatures for some months (e.g., maximum temperatures are underestimated in August
490 while overestimated in September). We also confirm that the cross-correlations of all three
491 variables for calendar months are fairly preserved in the simulations (not shown). The
492 performance confirms that the weather generator used in this study is appropriate to reproduce
493 climate scenarios for our study basins.

494



495 Figure 5 shows observed daily streamflow for the last three years of calibration and two years
496 in the validation period. Note that different calibration and validation periods are selected for
497 each basin due to the imbalance in the records of hydrologic data (see Section 3.2). For the
498 Boryeong Basin, augmented SAC-SMA is calibrated (validated) by using the observed daily
499 data from January 1999 to December 2013 (January 2014 to December 2018). The KGE, NSE,
500 and percent bias (PB) are 0.79, 0.58, and 0.2% for the calibration period and 0.77, 0.61, and
501 0.8% for the validation period, respectively. The PB is expressed as a percentage of observed
502 values. For the Beakje Basin, SAC-SMA is calibrated (validated) by using the data from
503 January 2013 to December 2016 (January 2017 to December 2018). The KGE, NSE, and PB
504 equal 0.83, 0.66, and 0.5% for the calibration period and 0.75, 0.55, and -8.3% for the validation
505 period. Based on performance criterion suggested by Martinez and Gupta (2010) and Moriasi
506 et al. (2007), these performances are considered either “good” or “efficient” for daily
507 simulation. Note that because the NSE is not adopted for the objective of calibration, it is not
508 significantly decreased from the calibration to the validation period. The parameters calibrated
509 for the two basins are also presented in Table 1.

510

511 *4.3 Rule curve comparison in historical period*

512 Figure 6 shows a time-series of Boryeong Reservoir storage operated by three rule curves
513 (C_{Base} , $C_{Forecast}$, and $C_{Dynamic}$) as well as three rule curves themselves for the most
514 recent seven years (2012-2018). This period is selected since it reflects the worst drought on
515 record (see Section 3.1). Note that simulated inflow for the Beakje Weir is utilized for
516 $C_{Dynamic}$ based on the assumption that the water transfer option is available from the initial
517 date of the Boryeong Reservoir. Figure 6a presents the status quo operation curves exhibiting



518 a pronounced and seasonal pattern whereas Figures 6b and 6c also show the forecast-based rule
519 curves which are changed year to year on the basis of a hydrologic forecast associated with
520 lagged ENSO events. Here, Niño 3.4⁺ $C_{Forecast}$ is shifted downward especially for the
521 severe storage level (C^{**}) compared to Niño 3.4⁻ $C_{Forecast}$ which is consistent with the
522 ENSO forecasting signal identified in Section 4.1.

523

524 Several insights emerge from Figure 6. In Figures 6a, C_{Basehe} experiences critical
525 drawdowns during the 2016-2017 drought event with storage falling below C^{***} for 272 days.
526 Under $C_{Forecast}$, critical drawdowns are somewhat moderated with storage falling below C^{***}
527 for 243 days albeit with little benefit. The marginal improvement is from a potential drawback
528 of the forecast-based operation. In 2017 when the drought was most severe, the risk of water
529 shortage is incorrectly predicted by the summer ENSO, leading to the storage level falling
530 below the critical level. That highlights that the risk associated with seasonal forecasts in an
531 individual year can increase even if average performance is better from reliable forecast
532 information. A potential drawback is alleviated when the real-option water transfer is adopted
533 ($C_{Dynamic}$). The real-option from the Beakje Weir eliminates critical drawdowns even in 2016-
534 2017 which are the driest periods on record. This indicates that the real-option is beneficial in
535 preventing the Boryeong Reservoir from falling below critical storage levels even for a multi-
536 year drought event.

537

538 4.4 Robustness in climate uncertainties

539 Figure 7 shows the RI of three operation rule curves (C_{Basehe} , $C_{Forecast}$, and $C_{Dynamic}$) for



540 changes in mean precipitation and temperature with the teleconnection forecast skill held at
541 baseline level ($\rho=0.55$). $C_{Baseline}$ provides robust performance for all temperature changes
542 when mean precipitations exceed 110% of historical means but when mean precipitations drop,
543 the operation is fairly vulnerable. In addition, the operation rule is not robust for current
544 precipitation and temperature conditions ($RI = 0.71$). On the other hand, $C_{Forecast}$ shows
545 improved performance for current conditions ($RI = 0.83$). In comparison, $C_{Forecast}$
546 improves overall system performance compared to $C_{Baseline}$, suggesting that improved
547 operation performance is expected when the forecast-based operation is applied as described
548 in previous studies (Block, 2011; Visser, 2017). When $C_{Dynamic}$ is utilized, we may expect
549 more reliable performance, which is confirmed in the analysis using historical records. Even
550 though mean precipitation is reduced by 10% of the historic value, a high level of robustness
551 ($RI= 0.90$) could be expected by $C_{Dynamic}$, supporting the use of option instruments for the
552 Boryeong reservoir.

553

554 In the results, we also confirm nonlinear results by changes in mean temperature whereas
555 changes in mean precipitation lead to consistently dominant changes. The nonlinear
556 performance in warmer conditions may be due to a shift in the hydrograph that accompanies
557 changes in temperature due to changes in the timing and magnitude of snow accumulation and
558 melting. Figure 7 also includes pdfs developed by an ensemble of GCM projections.
559 Projections are centered on an increase of 11% mean precipitation and 1.78 °C. For the
560 centered projections, three operation rules achieve a similarly reliable performance. However,
561 approximately 38% (25%) of the GCM projections are located in the relatively risky climate
562 surfaces for $C_{Baseline}$ ($C_{Dynamic}$). The portion of the GCM (11%) is further decreased for



563 $C_{Dynamic}$. Taken together, an improved operation rule may be urgently needed and can be
564 achieved by our dynamic operation rule if teleconnection forecast skills are preserved.

565

566 Next, Figure 8 summarizes the results for all of the combinations of climate change considered
567 in this study. Also, the DRI is calculated for each forecast skill (see Section 2.3) and is
568 presented in Table 1. Note that the status quo operation is not shown here because it is not
569 affected by degradation of the forecast skill therefore the results of Figure 7a are equally
570 obtained for each forecast skill. Several insights emerge from these results. First, the robustness
571 of two dynamic operations, $C_{Forecast}$ and $C_{Dynamic}$, are decreased when the forecast skill
572 abilities decline. Second, $C_{Forecast}$ provides adequate performance across a wide range of the
573 forecast skill degradation when compared to $C_{Baseline}$ (DRI = 0.632). This also includes
574 very low forecast ability ($\rho = 0.15$) although the results may be caused by the higher reservoir
575 levels used in $C_{Forecast}$ than in $C_{Baseline}$ (see Figure 6). However, improved $C_{Forecast}$
576 does not still satisfy our predefined threshold (Λ^{DRI}) in all forecast skills. Third, $C_{Dynamic}$ is
577 very effective when the forecast-based operation is incorporated with the real-option water
578 transfer. $C_{Dynamic}$ shows the reliable robustness (DRI = 0.706) even with lower forecast
579 ability ($\rho = 0.35$) for the forecast-based operation. It suggests that the real-option can manage
580 both the downside risk of faulty seasonal forecasts and severe changes in climate. These results
581 advocate the use of the real-option for the Boryeong Reservoir as a powerful instrument in the
582 future. We note that the economic analysis to maintain infrastructure to facilitate water transfers
583 is not conducted in this study. However, the cost may be significantly less than those required
584 to install a new impoundment to expand system storage, which is another advantage for the



585 real option. Lastly, we may conclude that $C_{Dynamic}$ is quite robust even though the forecast
586 skill ability is significantly reduced by 40% of the current skill.

587

588 **5. Summary and Conclusions**

589 Dynamic reservoir operations have received widespread interest in the field of reservoir
590 operations and climate change adaptation strategy, but little attention to quantifying their
591 robustness to a variety of climate uncertainties. Using a robustness-based method, we develop
592 an evaluation framework that can be applied based on a range of defined climate change space
593 over which acceptable performance can be achieved. In particular, a new metric, the
594 degradation robustness index (DRI), is proposed to scrutinize the robustness of a forecast-based
595 operation rule under the possibility of forecast skill degradation and climate variable alterations.

596

597 The novel contribution is also achieved by proposing new dynamic reservoir operation rules
598 for our case study, the Boryeong Reservoir, which has recently experienced the worst drought
599 in its historical record. For developing forecast-based operations, we newly identify lagged
600 ENSO effects on inflows during early spring the most crucial period for the Boryeong operation.
601 The comparative results suggest that a forecast-based operation may be favorable compared to
602 the status quo operation currently utilized in the reservoir system. In addition, we also examine
603 the effects of a water transfer option that recently questioned whether a real-option water
604 transfer from the Baekje Weir is useful. Using such an option would bolster system
605 performance by enabling the reallocation of water when the Boryeong Reservoir is in a
606 precarious condition. Furthermore, we confirm the real-option can support a forecast-based
607 operation for our reservoir system when ill-informed operation adjustments would be happened
608 by misguided climate information.



609

610 There are opportunities to further extend our evaluation. To simplify the analysis, we assume
611 that current water demand scenarios will persist under future climate changes. While this
612 simple assumption is acceptable for this study, future work needs to explore the impacts of
613 various water demand scenarios (e.g., expansion of irrigation). Also, hydrologic uncertainty is
614 not considered here even if the uncertainty may be significant for reservoir operations focusing
615 on water supply objectives (Marton and Paseka, 2017; Steinschneider et al., 2015). A forecast-
616 based operation could be designed to better utilize seasonal forecast information by using a
617 specific optimization algorithm (e.g., Denaro et al. (2017)). However, the optimized operation
618 policies should be re-evaluated in a cross-validation framework to ensure the calibration sets
619 are robust. Given that only the relatively limited hydrologic data is available in our case study
620 (21 years), the optimized policies is not considered.

621

622 Our framework is rather computationally intensive because a large set of future ensemble
623 scenarios is employed to represent natural fluctuations in climate uncertainties. The limitation
624 may be acceptable since the mandatory simulation time could be prohibitive for multi-reservoir
625 systems, and thus high performance computing may be required (Kasprzyk et al., 2013).
626 However, local water managers may prefer simple and concise techniques for their practical
627 management. Future work could address devising concise approaches, which could effectively
628 reduce computational burden.

629

630 In addition to the urgent need for effective reservoir operations, the western Geum River Basin
631 has also faced many water-related issues including controlling water quality and combatting
632 eutrophication from rising water temperature (Ahn and Kim, 2019). Perhaps, the most essential



633 research is to estimate local streamflow after taking into account the impacts of water
634 withdrawal networks. Although our study basin, the Boryeong Basin, is relatively free from
635 human adjustments, most parts of the western Geum River Basin are regulated, indicating that
636 relying on traditional hydrological models without accounting for human activity modules may
637 not accurately represent the regional hydrology. Therefore, a network of hydrological models
638 with feedback in coupled local reservoirs (e.g., Lv et al. (2016)) is required for hydrologic
639 analysis. We believe that such large-scale coupled hydrologic and system models will be an
640 attractive avenue for future research.

641

642

Acknowledgements

643 This work was supported by the National Research Foundation of Korea (NRF) grant funded
644 by the Korea government (MSIT) (No. 2019R1C1C1002438). The authors would like to thank
645 Byoung-Dong Oh at the Korean Water Resources Corporation for providing data of the
646 Boryeong Reservoir and Beakje Weir during the development of this paper. We also appreciate
647 the APEC Climate Center (APCC) for offering the downscaled climate projections.

648

649

REFERENCES

- 650 Aboutalebi, M., Bozorg Haddad, O. and Loaiciga, H. A.: Optimal monthly reservoir operation
651 rules for hydropower generation derived with SVR-NSGAIL, *J. Water Resour. Plan. Manag.*,
652 141(11), 04015029, 2015.
- 653 Ahmad, A., El-Shafie, A., Razali, S. F. M. and Mohamad, Z. S.: Reservoir optimization in water
654 resources: a review, *Water Resour. Manag.*, 28(11), 3391–3405, 2014.
- 655 Ahn, K.-H. and Kim, Y.-O.: Incorporating Climate Model Similarities and Hydrologic Error
656 Models to Quantify Climate Change Impacts on Future Riverine Flood Risk, *J. Hydrol.*, 2019.
- 657 Ahn, K.-H., Merwade, V., Ojha, C. S. P. and Palmer, R.: Quantifying Relative Uncertainties in
658 the Detection and Attribution of Human-induced Climate Change on Winter Streamflow, *J.*



- 659 Hydrol., 2016.
- 660 Akaike, H.: Likelihood of a model and information criteria, *J. Econom.*, 16(1), 3–14, 1981.
- 661 Allan, A. M., Hostetler, S. W. and Alder, J. R.: Analysis of the present and future winter Pacific-
662 North American teleconnection in the ECHAM5 global and RegCM3 regional climate models,
663 *Clim. Dyn.*, 42(5–6), 1671–1682, 2014.
- 664 Allen, R. G., Pereira, L. S., Raes, D., Smith, M. and others: Crop evapotranspiration-Guidelines
665 for computing crop water requirements-FAO Irrigation and drainage paper 56, FAO Rome, 300,
666 6541, 1998.
- 667 Ashbolt, S. C. and Perera, B.: Multiobjective Optimization of Seasonal Operating Rules for
668 Water Grids Using Streamflow Forecast Information, *J. Water Resour. Plan. Manag.*, 144(4),
669 05018003, 2018.
- 670 Bai, Y., Wang, P., Xie, J., Li, J. and Li, C.: Additive model for monthly reservoir inflow forecast,
671 *J. Hydrol. Eng.*, 20(7), 04014079, 2014.
- 672 Block, P.: Tailoring seasonal climate forecasts for hydropower operations, *Hydrol. Earth Syst.*
673 *Sci.*, 15(4), 1355–1368, 2011.
- 674 Broad, K., Pfaff, A., Taddei, R., Sankarasubramanian, A., Lall, U. and de Souza Filho, F. de A.:
675 Climate, stream flow prediction and water management in northeast Brazil: societal trends and
676 forecast value, *Clim. Change*, 84(2), 217–239, 2007.
- 677 Brown, C. and Wilby, R. L.: An alternate approach to assessing climate risks, *Eos Trans. Am.*
678 *Geophys. Union*, 93(41), 401–402, 2012.
- 679 Brown, C., Werick, W., Leger, W. and Fay, D.: A decision-analytic approach to managing
680 climate risks: Application to the Upper Great Lakes, *JAWRA J. Am. Water Resour. Assoc.*,
681 47(3), 524–534, 2011.
- 682 Brown, C., Ghile, Y., Laverty, M. and Li, K.: Decision scaling: Linking bottom-up vulnerability
683 analysis with climate projections in the water sector, *Water Resour. Res.*, 48(9), 2012.
- 684 Bürger, G., Sobie, S., Cannon, A., Werner, A. and Murdock, T.: Downscaling extremes: An
685 intercomparison of multiple methods for future climate, *J. Clim.*, 26(10), 3429–3449, 2013.
- 686 Burnash, R.: The National Weather Service river forecast system–catchment model, *Water*
687 *Resources Publications.*, 1995.
- 688 Burnash, R. J., Ferral, R. L. and McGuire, R. A.: A generalized streamflow simulation system,
689 conceptual modeling for digital computers, 1973.
- 690 Chu, W., Gao, X. and Sorooshian, S.: Improving the shuffled complex evolution scheme for
691 optimization of complex nonlinear hydrological systems: Application to the calibration of the
692 Sacramento soil-moisture accounting model, *Water Resour. Res.*, 46(9), 2010.
- 693 Cordano, E. and Eccel, E.: Tools for stochastic weather series generation in R environment,



- 694 Ital. J. Agrometeorol.-Riv. Ital. Agrometeorol., 21(3), 31–42, 2016.
- 695 Denaro, S., Anghileri, D., Giuliani, M. and Castelletti, A.: Informing the operations of water
696 reservoirs over multiple temporal scales by direct use of hydro-meteorological data, *Adv. Water*
697 *Resour.*, 103, 51–63, 2017.
- 698 Eum, H.-I. and Cannon, A. J.: Intercomparison of projected changes in climate extremes for
699 South Korea: application of trend preserving statistical downscaling methods to the CMIP5
700 ensemble, *Int. J. Climatol.*, 37(8), 3381–3397, 2017.
- 701 Field, C. B., Barros, V., Stocker, T. F. and Dahe, Q.: Managing the risks of extreme events and
702 disasters to advance climate change adaptation: special report of the intergovernmental panel
703 on climate change, Cambridge University Press., 2012.
- 704 Fowler, H., Kilsby, C. and O’Connell, P.: Modeling the impacts of climatic change and
705 variability on the reliability, resilience, and vulnerability of a water resource system, *Water*
706 *Resour. Res.*, 39(8), 2003.
- 707 Gergis, J. L. and Fowler, A. M.: Classification of synchronous oceanic and atmospheric El
708 Niño-Southern Oscillation (ENSO) events for palaeoclimate reconstruction, *Int. J. Climatol.*,
709 25(12), 1541–1565, 2005.
- 710 Ghile, Y. B., Taner, M., Brown, C., Grijzen, J. and Talbi, A.: Bottom-up climate risk assessment
711 of infrastructure investment in the Niger River Basin, *Clim. Change*, 122(1–2), 97–110, 2014.
- 712 Giuliani, M., Castelletti, A., Pianosi, F., Mason, E. and Reed, P. M.: Curses, tradeoffs, and
713 scalable management: Advancing evolutionary multiobjective direct policy search to improve
714 water reservoir operations, *J. Water Resour. Plan. Manag.*, 142(2), 04015050, 2015.
- 715 Golembesky, K., Sankarasubramanian, A. and Devineni, N.: Improved drought management
716 of Falls Lake Reservoir: Role of multimodel streamflow forecasts in setting up restrictions, *J.*
717 *Water Resour. Plan. Manag.*, 135(3), 188–197, 2009.
- 718 Gong, G., Wang, L., Condon, L., Shearman, A. and Lall, U.: A simple framework for
719 incorporating seasonal streamflow forecasts into existing water resource management
720 practices1, Wiley Online Library., 2010.
- 721 Guimarães, R. C. and Santos, E. G.: Principles of stochastic generation of hydrologic time
722 series for reservoir planning and design: Case study, *J. Hydrol. Eng.*, 16(11), 891–898, 2011.
- 723 Gupta, H. V., Kling, H., Yilmaz, K. K. and Martinez, G. F.: Decomposition of the mean squared
724 error and NSE performance criteria: Implications for improving hydrological modelling, *J.*
725 *Hydrol.*, 377(1), 80–91, 2009.
- 726 Hargreaves, G. H. and Samani, Z. A.: Estimating potential evapotranspiration, *J. Irrig. Drain.*
727 *Div.*, 108(3), 225–230, 1982.
- 728 Hashimoto, T., Stedinger, J. R. and Loucks, D. P.: Reliability, resiliency, and vulnerability
729 criteria for water resource system performance evaluation, *Water Resour. Res.*, 18(1), 14–20,
730 1982.



- 731 Hassanzadeh, E., Elshorbagy, A., Wheeler, H. and Gober, P.: A risk-based framework for water
732 resource management under changing water availability, policy options, and irrigation
733 expansion, *Adv. Water Resour.*, 94, 291–306, 2016.
- 734 Ho, C.-H., Lee, J.-Y., Ahn, M.-H. and Lee, H.-S.: A sudden change in summer rainfall
735 characteristics in Korea during the late 1970s, *Int. J. Climatol. J. R. Meteorol. Soc.*, 23(1), 117–
736 128, 2003.
- 737 Hong, I., Lee, J.-H. and Cho, H.-S.: National drought management framework for drought
738 preparedness in Korea (lessons from the 2014–2015 drought), *Water Policy*, wp2016015, 2016.
- 739 Huang, B., Thorne, P. W., Banzon, V. F., Boyer, T., Chepurin, G., Lawrimore, J. H., Menne, M.
740 J., Smith, T. M., Vose, R. S. and Zhang, H.-M.: Extended reconstructed sea surface temperature,
741 version 5 (ERSSTv5): upgrades, validations, and intercomparisons, *J. Clim.*, 30(20), 8179–
742 8205, 2017.
- 743 Huard, D. and Mailhot, A.: A Bayesian perspective on input uncertainty in model calibration:
744 Application to hydrological model “abc,” *Water Resour. Res.*, 42(7), 2006.
- 745 Ihm, S. H., Seo, S. B. and Kim, Y.-O.: Valuation of Water Resources Infrastructure Planning
746 from Climate Change Adaptation Perspective using Real Option Analysis, *KSCE J. Civ. Eng.*,
747 1–9, 2019.
- 748 Jang, S., Oh, K. and Oh, J.: Impacts on Water Surface Level of the Geum River with the
749 Diversion Tunnel Operation for Low Flow Augmentation of the Boryong Dam, *J. Environ. Sci.*
750 *Int.*, 26(9), 1031–1043, 2017.
- 751 Jeuland, M. and Whittington, D.: Water resources planning under climate change: Assessing
752 the robustness of real options for the Blue Nile, *Water Resour. Res.*, 50(3), 2086–2107, 2014.
- 753 Jin, X., Xu, C.-Y., Zhang, Q. and Singh, V.: Parameter and modeling uncertainty simulated by
754 GLUE and a formal Bayesian method for a conceptual hydrological model, *J. Hydrol.*, 383(3),
755 147–155, 2010.
- 756 Kasprzyk, J. R., Nataraj, S., Reed, P. M. and Lempert, R. J.: Many objective robust decision
757 making for complex environmental systems undergoing change, *Environ. Model. Softw.*, 42,
758 55–71, 2013.
- 759 Kim, J., Park, J., Jang, S., Kim, H. and Kang, H.: Improving Reservoir Operation Criteria to
760 Stabilize Water Supplies in a Multipurpose Dam: Focused on Nakdong River Basin in Korea,
761 *Water*, 10(9), 1236, 2018.
- 762 Kim, J.-S. and Jain, S.: Precipitation trends over the Korean peninsula: typhoon-induced
763 changes and a typology for characterizing climate-related risk, *Environ. Res. Lett.*, 6(3),
764 034033, 2011.
- 765 Kim, Y.-O., Ihm, S. H., Yoon, H. N. and Kim, G. J.: Analysis of economic feasibility of
766 Boryeong dam conduit construction due to uncertainty of drought occurrence, in *Korean
767 Society of Civil Engineers (KSCE) CONVENTION*, Busan, Korea., 2017.



- 768 Kohyama, T., Hartmann, D. L. and Battisti, D. S.: Weakening of nonlinear ENSO under global
769 warming, *Geophys. Res. Lett.*, 45(16), 8557–8567, 2018.
- 770 Korteling, B., Dessai, S. and Kapelan, Z.: Using information-gap decision theory for water
771 resources planning under severe uncertainty, *Water Resour. Manag.*, 27(4), 1149–1172, 2013.
- 772 Koutsoyiannis, D., Montanari, A., Lins, H. F. and Cohn, T. A.: Climate, hydrology and
773 freshwater: towards an interactive incorporation of hydrological experience into climate
774 research, 2009.
- 775 Kug, J.-S., Jin, F.-F. and An, S.-I.: Two types of El Niño events: cold tongue El Niño and warm
776 pool El Niño, *J. Clim.*, 22(6), 1499–1515, 2009.
- 777 Kwon, H.-H., Lall, U. and Kim, S.-J.: The unusual 2013–2015 drought in South Korea in the
778 context of a multcentury precipitation record: Inferences from a nonstationary, multivariate,
779 Bayesian copula model, *Geophys. Res. Lett.*, 43(16), 8534–8544, 2016.
- 780 Lee, J.-J., Kwon, H.-H. and Kim, T.-W.: Spatio-temporal analysis of extreme precipitation
781 regimes across South Korea and its application to regionalization, *J. Hydro-Environ. Res.*, 6(2),
782 101–110, 2012.
- 783 Lempert, R. J. and Groves, D. G.: Identifying and evaluating robust adaptive policy responses
784 to climate change for water management agencies in the American west, *Technol. Forecast.
785 Soc. Change*, 77(6), 960–974, 2010.
- 786 Li, L. and Xu, C.-Y.: The comparison of sensitivity analysis of hydrological uncertainty
787 estimates by GLUE and Bayesian method under the impact of precipitation errors, *Stoch.
788 Environ. Res. Risk Assess.*, 28(3), 491–504, 2014.
- 789 Liu, L., Cui, Y. and Luo, Y.: Integrated modeling of conjunctive water use in a canal-well
790 irrigation district in the lower Yellow River basin, China, *J. Irrig. Drain. Eng.*, 139(9), 775–784,
791 2013.
- 792 Lv, M., Hao, Z., Lin, Z., Ma, Z., Lv, M. and Wang, J.: Reservoir operation with feedback in a
793 coupled land surface and hydrologic model: a case study of the Huai River Basin, China,
794 *JAWRA J. Am. Water Resour. Assoc.*, 52(1), 168–183, 2016.
- 795 Martinez, G. F. and Gupta, H. V.: Toward improved identification of hydrological models: A
796 diagnostic evaluation of the “abcd” monthly water balance model for the conterminous United
797 States, *Water Resour. Res.*, 46(8), 2010.
- 798 Marton, D. and Paseka, S.: Uncertainty impact on water management analysis of open water
799 reservoir, *Environments*, 4(1), 10, 2017.
- 800 Matrosov, E. S., Woods, A. M. and Harou, J. J.: Robust decision making and info-gap decision
801 theory for water resource system planning, *J. Hydrol.*, 494, 43–58, 2013.
- 802 Ministry of Land, Infrastructure and Transport: Standard of water supply regulation to cope
803 with water shortage., 2015.



- 804 Moriasi, D., Arnold, J., Van Liew, M., Bingner, R., Harmel, R. and Veith, T.: Model Evaluation
805 Guidelines for Systematic Quantification of Accuracy in Watershed Simulations, *Trans.*
806 *ASABE*, 50(3), 885–900, 2007.
- 807 Mullen, K. M., Ardia, D., Gil, D. L., Windover, D. and Cline, J.: DEoptim: An R package for
808 global optimization by differential evolution, 2009.
- 809 Najafi, M., Moradkhani, H. and Jung, I.: Assessing the uncertainties of hydrologic model
810 selection in climate change impact studies, *Hydrol. Process.*, 25(18), 2814–2826, 2011.
- 811 Najibi, N., Devineni, N. and Lu, M.: Hydroclimate drivers and atmospheric teleconnections of
812 long duration floods: An application to large reservoirs in the Missouri River Basin, *Adv. Water*
813 *Resour.*, 100, 153–167, 2017.
- 814 Padowski, J. C., Gorelick, S. M., Thompson, B. H., Rozelle, S. and Fendorf, S.: Assessment of
815 human–natural system characteristics influencing global freshwater supply vulnerability,
816 *Environ. Res. Lett.*, 10(10), 104014, 2015.
- 817 Palmer, R. N. and Characklis, G. W.: Reducing the costs of meeting regional water demand
818 through risk-based transfer agreements, *J. Environ. Manage.*, 90(5), 1703–1714, 2009.
- 819 Pfaff, B.: *Analysis of integrated and cointegrated time series with R*, Springer Science &
820 *Business Media*, 2008.
- 821 Revilla-Romero, B., Beck, H. E., Burek, P., Salamon, P., de Roo, A. and Thielen, J.: Filling the
822 gaps: Calibrating a rainfall-runoff model using satellite-derived surface water extent, *Remote*
823 *Sens. Environ.*, 171, 118–131, 2015.
- 824 Romsdahl, R. J.: Decision support for climate change adaptation planning in the US: why it
825 needs a coordinated internet-based practitioners’ network, *Clim. Change*, 106(4), 507–536,
826 2011.
- 827 Sankarasubramanian, A., Lall, U., Devineni, N. and Espinueva, S.: The role of monthly updated
828 climate forecasts in improving intraseasonal water allocation, *J. Appl. Meteorol. Climatol.*,
829 48(7), 1464–1482, 2009.
- 830 Schewe, J., Heinke, J., Gerten, D., Haddeland, I., Arnell, N. W., Clark, D. B., Dankers, R.,
831 Eisner, S., Fekete, B. M., Colón-González, F. J. and others: Multimodel assessment of water
832 scarcity under climate change, *Proc. Natl. Acad. Sci.*, 111(9), 3245–3250, 2014.
- 833 Sharma, S., Srivastava, P., Fang, X. and Kalin, L.: Hydrologic simulation approach for El Niño
834 Southern Oscillation (ENSO)-affected watershed with limited raingauge stations, *Hydrol. Sci.*
835 *J.*, 61(6), 991–1000, 2016.
- 836 Singh, A., Panda, S. N., Saxena, C., Verma, C., Uzokwe, V. N., Krause, P. and Gupta, S.:
837 Optimization modeling for conjunctive use planning of surface water and groundwater for
838 irrigation, *J. Irrig. Drain. Eng.*, 142(3), 04015060, 2015.
- 839 Sohn, S.-J., Ahn, J.-B. and Tam, C.-Y.: Six month-lead downscaling prediction of winter to
840 spring drought in South Korea based on a multimodel ensemble, *Geophys. Res. Lett.*, 40(3),



- 841 579–583, 2013.
- 842 Steinschneider, S. and Brown, C.: Dynamic reservoir management with real-option risk
843 hedging as a robust adaptation to nonstationary climate, *Water Resour. Res.*, 48(5), 2012.
- 844 Steinschneider, S., McCrary, R., Wi, S., Mulligan, K., Mearns, L. O. and Brown, C.: Expanded
845 decision-scaling framework to select robust long-term water-system plans under hydroclimatic
846 uncertainties, *J. Water Resour. Plan. Manag.*, 141(11), 04015023, 2015.
- 847 Thiessen, A. H.: Precipitation averages for large areas, *Mon. Weather Rev.*, 39(7), 1082–1089,
848 1911.
- 849 Tsai, W.-P., Chang, F.-J., Chang, L.-C. and Herricks, E. E.: AI techniques for optimizing multi-
850 objective reservoir operation upon human and riverine ecosystem demands, *J. Hydrol.*, 530,
851 634–644, 2015.
- 852 Turner, S. W., Marlow, D., Ekström, M., Rhodes, B. G., Kularathna, U. and Jeffrey, P. J.:
853 Linking climate projections to performance: A yield-based decision scaling assessment of a
854 large urban water resources system, *Water Resour. Res.*, 50(4), 3553–3567, 2014.
- 855 Visser, J.: Evaluation of Seasonal Inflow Forecasting to Support Multipurpose Reservoir
856 Management: A case study for the Upper Maule River Basin, Chile, 2017.
- 857 Wang, H. and Fu, R.: Winter monthly mean atmospheric anomalies over the North Pacific and
858 North America associated with El Niño SSTs, *J. Clim.*, 13(19), 3435–3447, 2000.
- 859 Ward, P. J., Jongman, B., Kummu, M., Dettinger, M. D., Weiland, F. C. S. and Winsemius, H.
860 C.: Strong influence of El Niño Southern Oscillation on flood risk around the world, *Proc. Natl.
861 Acad. Sci.*, 111(44), 15659–15664, 2014.
- 862 Westphal, K. S., Laramie, R. L., Borgatti, D. and Stoops, R.: Drought management planning
863 with economic and risk factors, *J. Water Resour. Plan. Manag.*, 133(4), 351–362, 2007.
- 864 Whateley, S., Palmer, R. N. and Brown, C.: Seasonal hydroclimatic forecasts as innovations
865 and the challenges of adoption by water managers, *J. Water Resour. Plan. Manag.*, 141(5),
866 04014071, 2014.
- 867 Yan, H., Wei, W., Soon, W., An, Z., Zhou, W., Liu, Z., Wang, Y. and Carter, R. M.: Dynamics
868 of the intertropical convergence zone over the western Pacific during the Little Ice Age, *Nat.
869 Geosci.*, 8(4), 315, 2015.
- 870 Yang, T., Gao, X., Sellars, S. L. and Sorooshian, S.: Improving the multi-objective evolutionary
871 optimization algorithm for hydropower reservoir operations in the California Oroville–
872 Thermalito complex, *Environ. Model. Softw.*, 69, 262–279, 2015.
- 873 Yao, H. and Georgakakos, A.: Assessment of Folsom Lake response to historical and potential
874 future climate scenarios: 2. Reservoir management, *J. Hydrol.*, 249(1–4), 176–196, 2001.
- 875 Yoon, S. and Lee, T.: Investigation of hydrological variability in the Korean Peninsula with the
876 ENSO teleconnections, *Proc. Int. Assoc. Hydrol. Sci.*, 374, 165–173, 2016.



877 Zeff, H. B., Herman, J. D., Reed, P. M. and Characklis, G. W.: Cooperative drought adaptation:
878 Integrating infrastructure development, conservation, and water transfers into adaptive policy
879 pathways, *Water Resour. Res.*, 52(9), 7327–7346, 2016.

880 Zhang, J., Li, Y., Huang, G., Wang, C. and Cheng, G.: Evaluation of Uncertainties in Input Data
881 and Parameters of a Hydrological Model Using a Bayesian Framework: A Case Study of a
882 Snowmelt–Precipitation-Driven Watershed, *J. Hydrometeorol.*, 17(8), 2333–2350, 2016.

883 Zhang, W., Liu, P., Wang, H., Chen, J., Lei, X. and Feng, M.: Reservoir adaptive operating
884 rules based on both of historical streamflow and future projections, *J. Hydrol.*, 553, 691–707,
885 2017.

886 Zhao, T., Yang, D., Cai, X., Zhao, J. and Wang, H.: Identifying effective forecast horizon for
887 real-time reservoir operation under a limited inflow forecast, *Water Resour. Res.*, 48(1), 2012.

888 Zhu, T., Marques, G. F. and Lund, J. R.: Hydroeconomic optimization of integrated water
889 management and transfers under stochastic surface water supply, *Water Resour. Res.*, 51(5),
890 3568–3587, 2015.

891

892

893

894

895

896

897

898

899

900

901

902

903

904

905



906

907 **List of Figures**

908 Figure 1 Map of the Geum River basin and the two Reservoirs (Boryeong Reservoir and
909 Beakje Weir). Inset: the location of our study area in the Korean peninsula is
910 presented.

911

912 Figure 2 Standard operation rule curves currently used for the Boryeong reservoir.

913

914 Figure 3 Pearson correlation coefficients between seasonal SSTs in JJA at each grid cell
915 and (a) averaged FMA streamflow (c) FMA low flows in the following years, and
916 Box plots for (b) averaged FMA streamflow (d) FMA low flows during previous
917 years in which the JJA Nino 3.4 index is above or below its seasonal median.

918

919 Figure 4 Evaluation of historical climate simulations for the Boryeong and Beakje Basins,
920 including the (a) average (b) standard deviation (c) skewness (d) kurtosis (e)
921 average and (f) standard deviation for maximum and minimum temperatures.
922 Simulations for the Beakje Basin are highlighted (gray color). Also, observed
923 precipitation, maximum and minimum temperatures are shown by using three
924 colors (blue, red, and yellow).

925

926 Figure 5 Simulated and observed inflows over the calibration (left) and validation (right)
927 periods (a) for the Boryeong reservoir and (b) for the Beakje reservoir. Basin
928 precipitation is also presented.

929

930 Figure 6 Storage simulation (Black line) of the Boryeong reservoir over historical data
931 (2012- 2018) using (a) status quo operation rule, (b) forecast-based operation, and
932 (c) forecast-based operation with the real-option water transfer from the Beakje
933 Weir. The critical storage level (C^{***}) is commonly employed in three strategies.

934

935 Figure 7 Robustness of three operation rules (C_{Base} , $C_{Forecast}$, and $C_{Dynamic}$) under
936 future changes in precipitation and temperature with historical forecast skill ability
937 ($\rho=0.55$). The green color indicates the operation rule may be robust for the
938 defined changes. PDFs from GCM projections are superimposed over climate
939 space to present the likelihood of different climate changes.

940

941 Figure 8 Robustness of two dynamic operation rules for changes in mean precipitation,
942 mean temperature, and forecast skill ability. Here, the green color indicates the
943 operation rule may be robust for the defined changes.

944

945

946

947



948 **List of Tables**

949

950 Table 1 The parameters of the augmented Sacramento Soil Moisture Accounting (SAC-
951 SMA) model used in this study

952

953 Table 2 Results of the degradation robustness index (DRI) under three operation rules
954 (C_{Base} , $C_{Forecast}$, and $C_{Dynamic}$). Acceptable values for the DRI are
955 italicized and bolded.

956

957

958

959

960

961

962

963

964

965

966

967

968

969

970

971

972

973

974

975

976

977

978

979

980

981

982

983

984

985

986

987

988

989

990

991

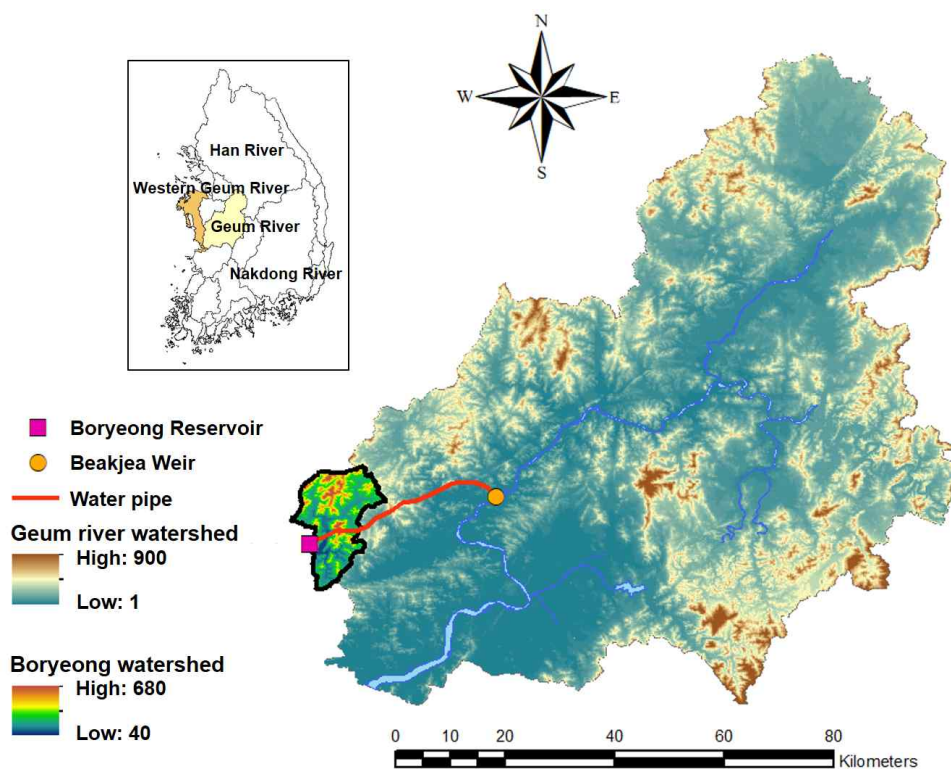
992

993

994



995

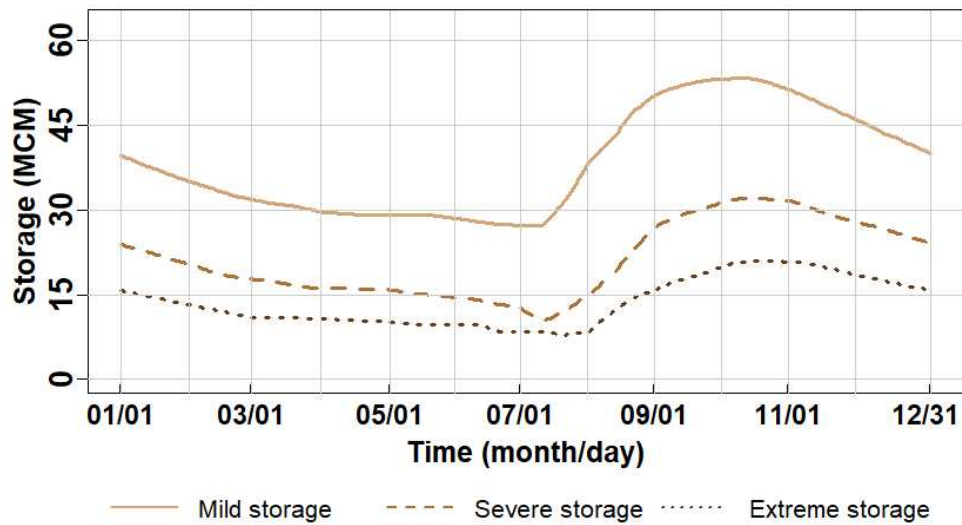


996
997
998
999
1000
1001
1002
1003
1004
1005
1006
1007
1008
1009
1010
1011
1012
1013
1014
1015
1016
1017

Figure 1 Map of the Geum River basin and the two Reservoirs (Boryeong Reservoir and Beakje Weir). Inset: the location of our study area in the Korean peninsula is presented.



1018

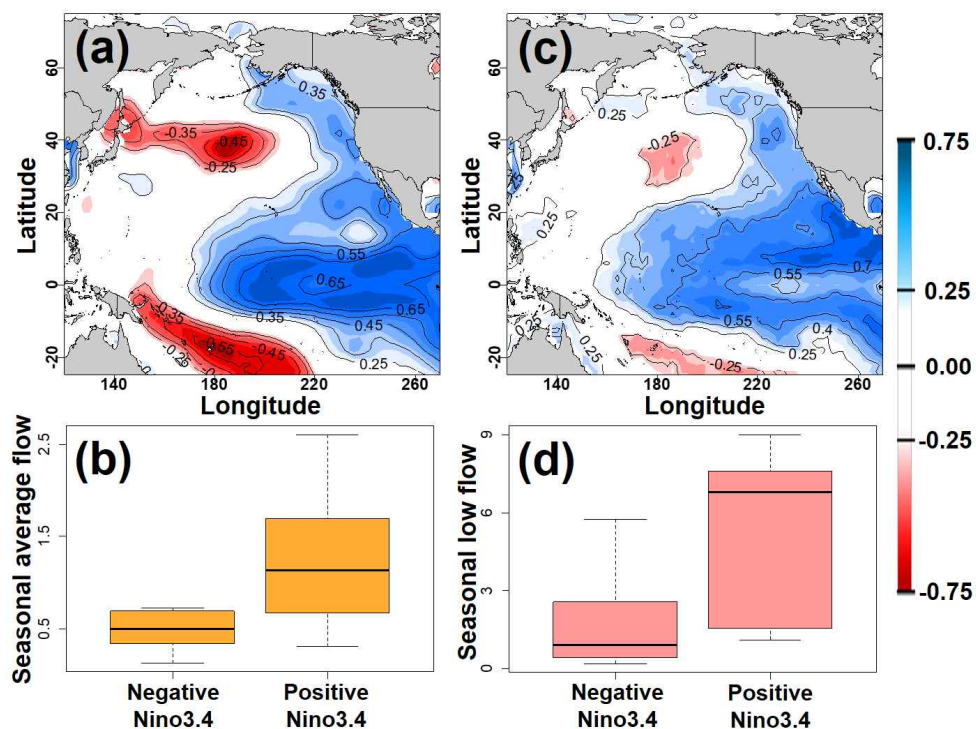


1019
1020 Figure 2 Standard operation rule curves currently used for the Boryeong reservoir.
1021

1022
1023
1024
1025
1026
1027
1028
1029
1030
1031
1032
1033
1034
1035
1036
1037
1038
1039
1040
1041
1042
1043
1044
1045
1046
1047
1048



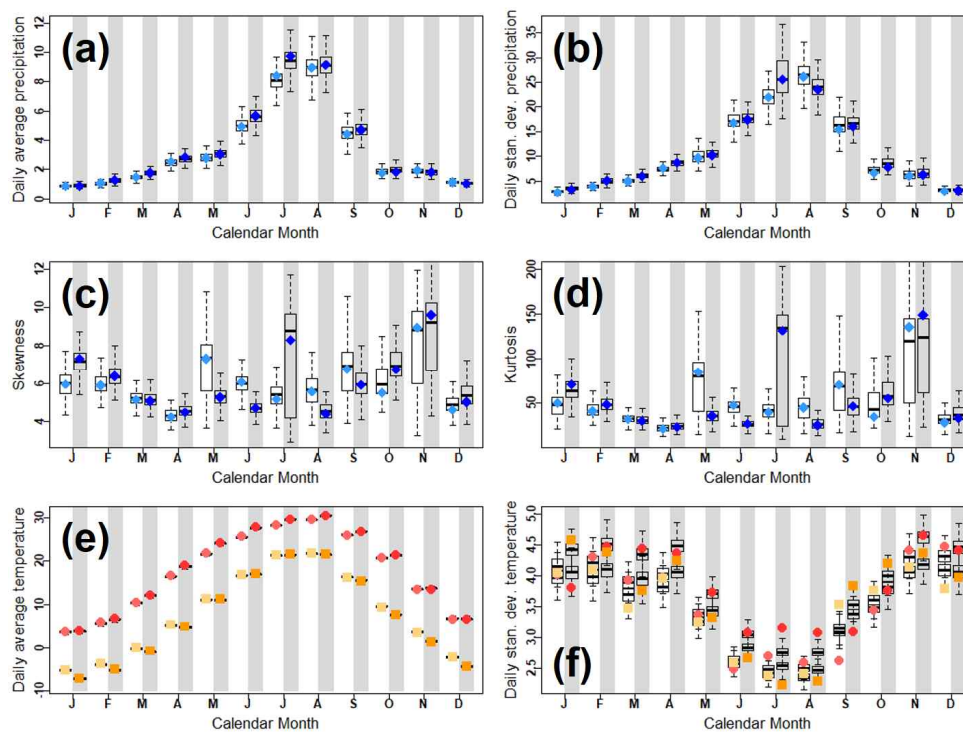
1049



1050
1051 Figure 3 Pearson correlation coefficients between seasonal SSTs in JJA at each grid cell and (a)
1052 averaged FMA streamflow (c) FMA low flows in the following years, and Box plots for (b)
1053 averaged FMA streamflow (d) FMA low flows during previous years in which the JJA Nino
1054 3.4 index is above or below its seasonal median.
1055
1056
1057
1058
1059
1060
1061
1062
1063
1064
1065
1066
1067
1068
1069
1070
1071
1072
1073



1074



1075

1076

1077

1078

1079

1080

1081

1082

1083

1084

1085

1086

1087

1088

1089

1090

1091

1092

1093

1094

1095

1096

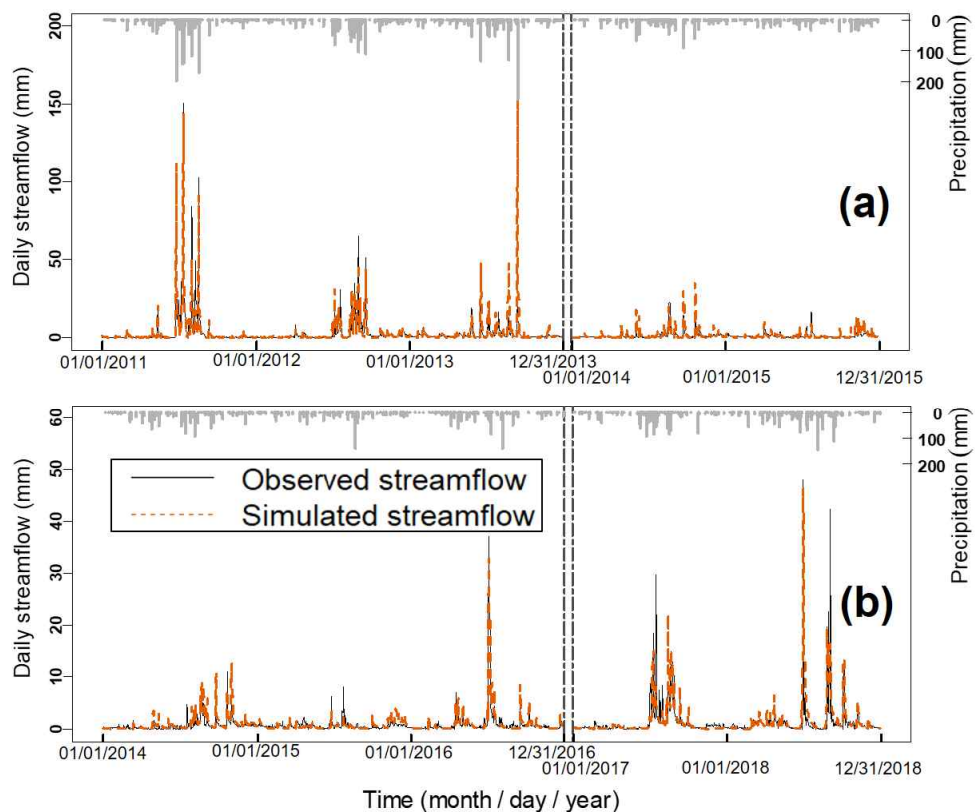
1097

1098

Figure 4 Evaluation of historical climate simulations for the Boryeong and Beakje Basins, including the (a) average (b) standard deviation (c) skewness (d) kurtosis (e) average and (f) standard deviation for maximum and minimum temperatures. Simulations for the Beakje Basin are highlighted (gray color). Also, observed precipitation, maximum and minimum temperatures are shown by using three colors (blue, red, and yellow).



1099

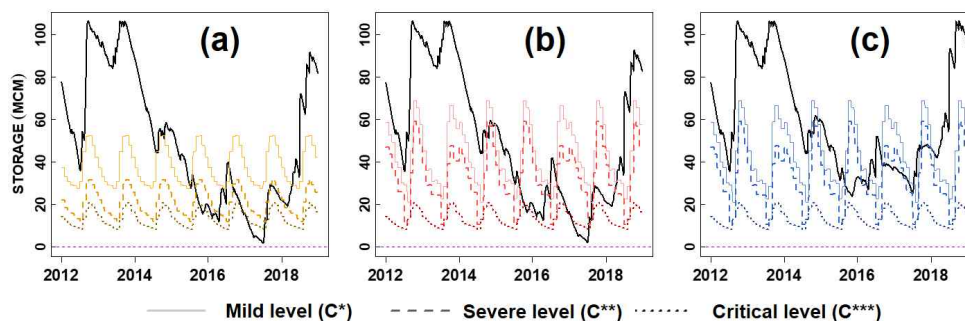


1100
1101 Figure 5 Simulated and observed inflows over the calibration (left) and validation (right)
1102 periods (a) for the Boryeong reservoir and (b) for the Beakje reservoir. Basin precipitation is
1103 also presented.

1104
1105
1106
1107
1108
1109
1110
1111
1112
1113
1114
1115
1116
1117
1118
1119
1120



1121

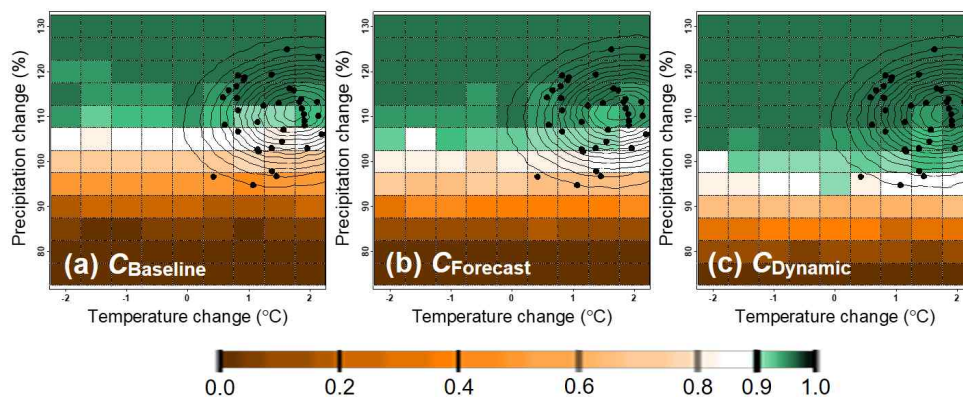


1122
1123
1124
1125
1126
1127
1128
1129
1130
1131
1132
1133
1134
1135
1136
1137
1138
1139
1140
1141
1142
1143
1144
1145
1146
1147
1148
1149
1150
1151
1152
1153
1154
1155
1156
1157
1158

Figure 6 Storage simulation (Black line) of the Boryeong reservoir over historical data (2012-2018) using (a) status quo operation rule, (b) forecast-based operation, and (c) forecast-based operation with the real-option water transfer from the Beakje Weir. The critical storage level (C^{***}) is commonly employed in three strategies.



1159



1160

1161

Figure 7 Robustness of three operation rules ($C_{Baseline}$, $C_{Forecast}$, and $C_{Dynamic}$) under future changes in precipitation and temperature with historical forecast skill ability ($\rho=0.55$). The green color indicates that the operation rule is robust for the defined changes. PDFs from GCM projections are superimposed over climate space to present the likelihood of different climate changes.

1165

1166

1167

1168

1169

1170

1171

1172

1173

1174

1175

1176

1177

1178

1179

1180

1181

1182

1183

1184

1185

1186

1187

1188

1189

1190

1191

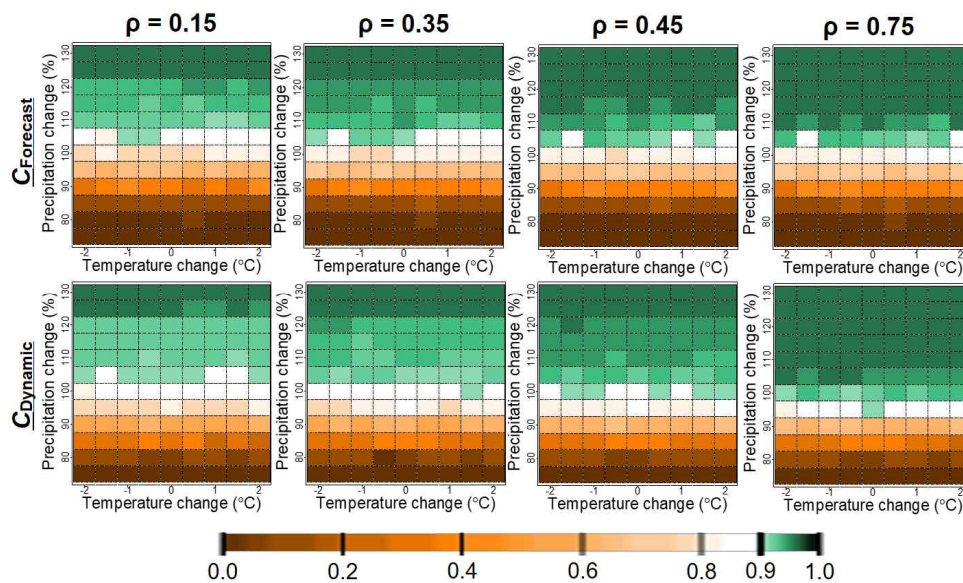
1192

1193

1194



1195



1196

1197

Figure 8 Robustness of two dynamic operation rules for changes in mean precipitation, mean temperature, and forecast skill ability. Here, the green color indicates that the operation rule is robust for the defined changes.

1200

1201

1202

1203

1204

1205

1206

1207

1208

1209

1210

1211

1212

1213

1214

1215

1216

1217

1218

1219

1220

1221

1222

1223

1224



1225 Table 1 The parameters of the augmented Sacramento Soil Moisture Accounting (SAC-SMA)
 1226 model used in this study
 1227

Parameter	Description	Range	Calibrated value	
			Boryeong	Beakje
UZTWM	Upper zone tension water capacity (mm)	(1 - 150)	5.80	3.30
UZFWM	Upper zone free water capacity (mm)	(1 - 150)	92.71	137.96
LZTWM	Lower zone tension water capacity (mm)	(1 - 500)	10.41	75.16
LZFPM	Lower zone primary free water capacity (mm)	(1 - 1000)	29.28	75.15
LZFSM	Lower zone supplementary free water capacity (mm)	(1 - 1000)	9.09	48.66
UZK	Upper zone free water lateral depletion rate (1/day)	(0.1 - 0.5)	0.50	0.31
LZPK	Lower zone primary free water depletion rate (1/day)	(0.0001-0.25)	0.00	0.10
LZSK	Lower zone supplementary free water depletion rate (1/day)	(0.01 - 0.25)	0.24	0.12
ZPERC	Percolation demand scale parameter	(1 - 250)	249.08	69.93
REXP	Percolation demand shape parameter	(0.0 - 5)	0.00	4.52
PFREE	Percolating water split parameter	(0.0 - 0.6)	0.03	0.23
PCTIM	Impervious fraction of the watershed area	(0.0 - 0.1)	0.10	0.00
ADIMP	Additional impervious areas	(0.0 - 0.4)	0.07	0.00
MLT	Snow melting parameter	(0.0 - 1.0)	0.66	0.36
TRAN	Temperature above which all precipitation falls as rain (°C)	(-3.0 - 3.0)	-2.93	-2.88
TDIF	Nonnegative temperature difference from the TRAN for water stored as snow (°C)	(0 - 3.0)	0.83	0.64
e_T	Error term for temperate	(-1.0 - 1.0)	0.97	0.98
e_P	Error term for precipitation	(0.95 - 1.05)	1.03	0.98
e_{PET}	Error term for evapotranspiration	(0.95 - 1.05)	1.04	1.03



1228

1229

1230

Table 2 Results of the degradation robustness index (DRI) under three operation rules (C_{Basehe} , $C_{Forecast}$, and $C_{Dynam \dot{t}}$). Acceptable values for the DRI are italicized and bolded.

Operations	C_{Basehe}	$C_{Forecast}$	$C_{Dynam \dot{t}}$
Forecast skill ability (ρ)	DRI		
0.15	0.632	0.634	0.693
0.35	0.632	0.647	<i>0.706</i>
0.45	0.632	0.655	<i>0.718</i>
0.55	0.632	0.660	<i>0.725</i>
0.75	0.632	0.675	<i>0.739</i>

1231

1232

1233

1234